Electron-hole interaction effects in the absorption spectra of phenylene-based conjugated polymers

Yu. N. Gartstein,* M. J. Rice,† and E. M. Conwell
Center for Photoinduced Charge Transfer, Chemistry Department, University of Rochester, Rochester, New York 14627 and Xerox Corporation, Wilson Center for Research and Technology, Mail Stop 114-21D, Webster, New York 14580
(Received 20 October 1994; revised manuscript received 20 January 1995)

A recently introduced microscopic model of the polyphenylenes is discussed and applied to study the absorption spectra of poly(paraphenylene) (PPP) and poly(phenylenevinylene) (PPV) oligomers. Emphasis is placed on the relation between the ultraviolet-visible spectra of oligomers and the effective electron-hole interaction potential. The long-range Coulomb interaction is treated on an equal footing with the intramonomer interactions. A physical understanding is achieved, within a single model, of the origin, polarization, positions, and intensities of the main absorption bands of short (biphenyl, stilbene) and long oligomers of PPP and PPV. For the infinite polymer chain the model leads to the generic appearance of three dispersing absorption bands. A fourth, dipole-forbidden, singlet excitation band is rendered allowed if charge-conjugation symmetry is broken. A family of four distinct, tightly bound, triplet state excitons is also found.

I. INTRODUCTION

The polyphenylenes form a wide and interesting class of organic semiconductors, including poly(paraphenylene) (PPP), poly(phenylenevinylene) (PPV), and the atomically bridged polyphenylenes such as polyaniline and poly(phenylene-oxide).[1–3] The essential qualitative physics of the photoexcitations of the polyphenylenes can be described by a simplified but analytically explicit microscopic model introduced in Ref. 4. This model considers the photoexcitations of the polymers as derived from the local ($e_{1g} \rightarrow e_{2u}$) excitations of the phenylene monomer. Among the effects the model incorporates, the most important are the "correlation-energy gaps" U_n between charged and charge-neutral excitations. U_n behave as an *effective* intramonomer electron-hole attraction and result, for the π-electron bandwidths $W \neq 0$, in the transfer of oscillator strength from interband transitions to exciton excitation. For the infinite polymer, the model accounts for the appearance of three main, dispersing, absorption bands whose relative spacings in energy are largely set by U_n and W (and corrected in interesting ways by long-range electron-hole attraction V_{eh} and dipole-dipole interaction V_{dd}). There is a fourth, dipole-forbidden, singlet excitation band which becomes allowed if charge-conjugation symmetry (CCS) is broken. The significance of the interrelation of these four bands, and that this interrelation provides immediate experimental information on the relative magnitudes of W and U_n, and, hence, on the relative importance of excitonic and interband excitation, appears not to have been previously recognized in the literature, to the best of our knowledge.

In this paper we present a more detailed study of the model of Rice and Gartstein[4] (hereafter referred to as RG), as applied both to long and short chains of polyphenylenes, and compare the results of calculations with available experimental data. Discussion of the model and the calculation method used for finite chains are given in Sec. II. In Sec. III results are obtained for the singlet excitations of the infinitely long oligomer, i.e., the polymer, using the analytical approach of Ref. 4. These reveal the family of four singlet excitation bands mentioned above. In the Appendix we extend this analytical theory to briefly consider the triplet state excitations of the model and we find a family of four distinct triplet excitons. In Secs. IV and V the RG model is applied to investigate the absorption spectra of finite chains of the *wide band* polyphenylenes, i.e., to PPP and PPV oligomers. Finite chains may be more representative of the experimental polymers than is the hypothetical (infinite) polymer. More important from the theoretical standpoint, however, is that for finite chains we treat the long-range Coulomb interaction V_{eh} exactly and hence on an equal footing with the intramonomer interactions U_n. The subsequent results obtained for longer chains (Sec. V) are in good agreement with those obtained by the analytical approach of Sec. III. Our results lead to a physical understanding, within a single model, not only of the origin, polarization, and positions of the main absorption bands of oligomers, but also of their *intensities*. In particular, we demonstrate that these features are determined by the details of the effective electron-hole interaction potential. Accordingly, by comparison with experiment, we are able to deduce approximate values for the microscopic parameters of the model. *Polarized* absorption experiments on molecular crystals of oligophenylenes would provide the means of obtaining more precise experimental values of these parameters.

An interesting finding of the present work is that the second and third prominent absorption bands in PPP, which have *different* polarizations, are found to approximately overlap in energy. In *unpolarized* absorption experiments, therefore, only two, rather than three, absorption bands would be resolved. This is consistent with the electron energy-loss studies[2,5] on PPP and more recent uv studies.[6] It is also consistent with the polarized absorption spectra of biphenyl.[7] Polarized reflectance study of

crystalline PPP should be able to resolve the second and third absorption bands of this polymer.

II. THE MODEL

The RG model considers a chain of N interacting phenylene monomers. Each monomer is assumed to have two degenerate (e_{1g}) hole states, labeled a and c, with excitation energy E_h, and two degenerate (e_{2u}) electron states, labeled b and d, with "excitation" energy E_e. Explicitly, their respective molecular orbitals (MO) are $\psi_a=(12)^{-1/2}\times(2,1,-1,-2,-1,1)$, $\psi_b=(12)^{-1/2}\times(-2,1,1,-2,1,1)$, $\psi_c=2^{-1}\times(0,-1,-1,0,1,1)$, and $\psi_d=2^{-1}\times(0,-1,1,0,-1,1)$, where each component of the MO specifies the atomic $C(2p)$ site amplitude in counterclockwise order starting from the carbon atom in the "left" *para* position (see Fig. 1 of Ref. 4). The singlet transitions between these MO are described by the operators $B^\dagger_{j\sigma}=b^\dagger_{j\sigma}a^\dagger_{j,-\sigma}$, $D^\dagger_{j\sigma}=d^\dagger_{j\sigma}c^\dagger_{j,-\sigma}$, $A^\dagger_{j\sigma}=d^\dagger_{j\sigma}a^\dagger_{j,-\sigma}$, and $C^\dagger_{j\sigma}=b^\dagger_{j\sigma}c^\dagger_{j,-\sigma}$, where the fermion operators $a^\dagger_{j\sigma}$, $b^\dagger_{j\sigma}$, $c^\dagger_{j\sigma}$, and $d^\dagger_{j\sigma}$, create, respectively, an electron or a hole with spin polarization σ in the specified MO of the monomer j ($j=1,\ldots,N$). They may be combined to form the four singlet excitations of the phenylene monomer:[8,9]

$$P^\dagger_{j,1}=\sum_\sigma (B^\dagger_{j\sigma}-D^\dagger_{j\sigma})/2\ ,\quad E_{1u}(x)\ ,$$

$$P^\dagger_{j,2}=\sum_\sigma (A^\dagger_{j\sigma}+C^\dagger_{j\sigma})/2\ ,\quad E_{1u}(y)\ ,$$

$$P^\dagger_{j,3}=\sum_\sigma (B^\dagger_{j\sigma}+D^\dagger_{j\sigma})/2\ ,\quad B_{1u}\ ,$$

$$P^\dagger_{j,4}=\sum_\sigma (A^\dagger_{j\sigma}-C^\dagger_{j\sigma})/2\ ,\quad B_{2u}\ .$$

The first and second E_{1u} excitations have transition dipole moments in the monomer x and y directions, respectively, while the B_{1u} and B_{2u} excitations are dipole forbidden.[8] We take the x axis to be the axis running through the two *para* carbon atoms of the phenylene monomer. In terms of these operators the Hamiltonian H defining the RG model is

$$H=\sum_{j\sigma}\{E_h(a^\dagger_{j\sigma}a_{j\sigma}+c^\dagger_{j\sigma}c_{j\sigma})+E_e(b^\dagger_{j\sigma}b_{j\sigma}+d^\dagger_{j\sigma}d_{j\sigma})\}+H_d+H_{ee}\ , \tag{1}$$

where

$$H_d=-\sum_{j\sigma}\{t_{bb}(b^\dagger_{j+1,\sigma}b_{j\sigma}+\text{H.c.})+t_{aa}(a^\dagger_{j+1,\sigma}a_{j\sigma}+\text{H.c.})+t_{ab}[(b^\dagger_{j+1,\sigma}-b^\dagger_{j-1,\sigma})a^\dagger_{j,-\sigma}+\text{H.c.}]\} \tag{2}$$

describes the delocalization of the b and a orbitals due to the intermolecular hopping integrals t, while

$$H_{ee}=-\sum_{jn}U_nP^\dagger_{jn}P_{jn}+V_{dd}+V_{eh} \tag{3}$$

specifies the leading contributions arising from Coulomb interactions. In the present paper we do not discuss electron-lattice interaction effects explicitly.

We note that in Eq. (2) there is no intermonomer hopping between the c and d orbitals so that these hole and electron orbitals remain localized. For application to PPV we note that the hopping integrals in H_d represent hopping processes over the vinylene units. Note, however, that the mixing between benzene and vinylene states is rather strong. The calculation in Ref. 10 showed that the band structures of the relevant bands in planar PPP and PPV are very similar and that the interband splitting in PPV is much smaller than the bandwidths.[11] In the context of electron delocalization, therefore, the PPP-type band structure is expected to be a good approximation for an *effective* model of PPV. In this paper we will use the PPP-type model for both polymers employing, however, different parameter values as appears appropriate. For this reason we will later take the polymer axis to coincide with the local phenylene x axis for PPV. Of course, for a more detailed description, the model can be extended to treat the vinylene states in PPV explicitly. For our analysis we will take $t_{aa}=t_{bb}=t_{ab}=t$, a constant, reflecting CCS of these systems. We note that for discussion for the atomically bridged polyphenylenes, which do *not* possess CCS, different effective site energies E^b_e, E^d_e, E^a_h, and E^c_h should be taken for the local orbital energies in Eq. (1) as well as $t_{aa}\neq t_{bb}$. The same should be done to take account of distortion of the phenylene monomer symmetry by side groups such as occurs in dimethoxy PPV and MEH-PPV.[12]

The first term in Eq. (3) gives the *energy gain* U_n when an electron and a hole in a singlet state are simultaneously present on the *same* monomer in the symmetry combination n. It is convenient to choose the one-electron energy reference point so that $E_e=E_h=\alpha_0$. Then it follows from the first terms of Eqs. (1) and (3) that the *local* monomer excitation energies are $E_n=2\alpha_0-U_n$. We expect these to depend mildly on the electronic polarizability of the environment while we expect both α_0 and U_n to depend much more significantly on this quantity. For the benzene molecule in the vapor, $U_1=U_2$, since $P^\dagger_{j1}$ and $P^\dagger_{j2}$ are symmetry doublets, and molecular spectroscopy gives[8,13,14] $E_1\simeq 6.8$–6.9 eV, $U_3-U_1\simeq 0.7$–0.8 eV, and $U_4-U_1\simeq 2.0$–2.2 eV (where the right-hand side of these results denotes the scatter in different measurements). Of course, in a medium the differences of U_n values can change from the values in benzene vapor, since the polarization of the environment can depend on the symmetry n. We will, however, see that making use of the benzene values of U_n-U_m already produces fairly good fits to experimental data. We note that for $U_1\neq U_3$ the first term of Eq. (3) leads to an intramonomer coupling of the $B^\dagger$ and $D^\dagger$ excitations while for $U_2\neq U_4$ it leads to a coupling of the $A^\dagger$ and $C^\dagger$ excitations. The benzene data indicate that these couplings are significant.

The second term of Eq. (3)

$$V_{dd}=-\sum_{jnm}V_{nm}(P^\dagger_{j+1,n}+P_{j+1,n})(P^\dagger_{jm}+P_{jm})\ , \tag{4}$$

describes the delocalization of the charge-neutral intramonomer excitations via the dipole-dipole interaction ($n,m\leq 2$). Its magnitude has been discussed in RG and it leads to small but interesting corrections to the relative positions of the absorption bands. A nonvanishing V_{nm}

will lead to dispersion of absorption bands in the ultraviolet which could be measured via electron energy-loss spectroscopy (EELS) experiments on high-quality crystalline films. For the narrow bandwidth polyphenylenes V_{dd} clearly becomes an important factor. For a planar PPP structure, the nonvanishing matrix elements are $V_{11} \equiv V_{xx} = V$ and $V_{22} \equiv V_{yy} = -V/2$, the model relationship we will use for demonstration in Figs. 3 and 5. In PPV, V_{dd} is supposed to occur virtually through the vinylene unit, and we will take the V_{xx} element as the only nonvanishing one in our calculations for stilbene and PPV. With only on-site and dipole-dipole interaction left in Eq. (3) our model resembles a simpler model introduced by Egri.[15]

The third term in Eq. (3) is the long-range Coulomb attraction V_{eh}, which is introduced as

$$V_{eh} = V_C \sum_{j \neq l} \rho_j \rho_l / 2|j-1| \ , \tag{5}$$

where $\rho_j = \sum_\sigma (a_{j\sigma}^\dagger a_{j\sigma} + c_{j\sigma}^\dagger c_{j\sigma} - b_{j\sigma}^\dagger b_{j\sigma} - d_{j\sigma}^\dagger d_{j\sigma})$ is the net charge density on the monomer j. For simplicity, in Eq. (5) no allowance is made for the different symmetries of the local electron and hole orbitals. (It is not difficult to introduce a dependence of V_{eh} on distribution of charges within monomers). The constant V_C is the interaction energy of charges on neighboring monomers and $E_{CT} = 2\alpha_0 - V_C$ may be considered to be the energy to create a "charge-transfer" exciton in the limit $t \to 0$. An estimate of V_C is provided by $V_C \simeq e^2/\epsilon d$, d being the monomer lattice spacing and ϵ the dielectric constant.

The absorption and EELS spectra of the model may be found by calculating the complex frequency- and wave-vector-dependent conductivity $\sigma_{\alpha\alpha}(Q,\omega)$ where $\alpha = x$ or y and Q denotes an arbitrary wave vector along the x direction. The RG H defined in Eq. (1) makes no assumptions about what the polymer axis is. For the present calculations, however, we take the polymer axis to coincide with the local phenylene x axis. In terms of eigenstates of our system the real part of the conductivity at zero temperature is expressed as follows:

$$\mathrm{Re}\sigma_{\alpha\alpha}(Q,\omega) = \pi (2Ab\omega)^{-1} \sum_\kappa |\langle \kappa | J_Q^\alpha | 0 \rangle|^2 \delta(E_\kappa - \hbar\omega) \ , \tag{6}$$

where A is the transverse area per chain and b the lattice constant of the chain. In Eq. (6) $|0\rangle$ denotes the ground state and $|\kappa\rangle$ an excited state with energy E_κ relative to the ground state. $J_Q^\alpha = \sum_j \exp(iQj) J_j^\alpha$ is the current fluctuation operator for the α direction, while J_j^α are the *interband* currents:

$$J_j^x = ie \left\{ v_0 (P_{j,1}^\dagger - P_{j,1}) + (v_1/2) \sum_\sigma [(b_{j+1,\sigma}^\dagger + b_{j-1,\sigma}^\dagger) a_{j,-\sigma}^\dagger - \text{H.c.}] \right\} , \tag{7}$$

$$J_j^y = ie \{ v_0 (P_{j,2}^\dagger - P_{j,2}) \} \ , \tag{8}$$

where v_0 arises from the transition dipole moments of the E_{1u} excitations and the v_1 term arises from the "oblique" interband hopping terms in H_d, i.e., the terms in Eq. (2) that create electron-hole pairs across adjacent monomers. This term brings additional oscillator strength to the x-polarized transitions in the chain of coupled monomers as compared to the y-polarized transitions. We note that intermonomer hopping breaks the local E_{1u} symmetry of the displacement current. For planar PPP simple MO theory yields[4] $v_1 = v_0/3$. More generally, the ratio v_1/v_0 may be regarded as a parameter of the model. Equations (7) and (8) are strictly applicable to planar PPP. For nonplanar PPP, the y-polarized absorption must be understood as the absorption for the polarizations perpendicular to the chain direction. In PPV there is a small but finite angle $\theta \simeq 9° - 10°$ between the monomer and polymer axes, and the true current operators must be linear combinations of Eqs. (7) and (8) weighted by $\cos\theta$ and $\sin\theta$. Since the results of calculations will be compared only with unpolarized absorption data for PPV, we do not consider these details here.

The full Hamiltonian (1) is a many-body Hamiltonian which must be simplified for the purposes of our study. An approximation we use consists in neglecting those terms of H that do not conserve the number of electron-hole pairs. Ignoring these terms is a reasonable approximation for large enough α_0. These are the terms in V_{dd} (4) that create and annihilate pairs of excitations and the oblique hopping terms in H_d (2). The latter terms are, however, necessarily retained in J_j^x in the form given by Eq. (7). The role of oblique terms will be discussed in more detail later. Here we just note that the relative correction to the energy levels from these terms is of the order $(t_{ab}/\alpha_0)^2 \lesssim 0.1$. What is more important, these corrections do not affect our important conclusions. The terms neglected in V_{dd} would produce (for the wide bandwidth polyphenylenes assumed here) even smaller corrections, namely, of the order $V/2\alpha_0$. For the Hamiltonian so truncated the problem of the evaluation of the eigenstates $|\kappa\rangle$ and eigenvalues E_κ, required for Eq. (6), reduces to the two-body problem of a single electron interacting with a single hole, which is treated exactly. Let us introduce $|\Phi\rangle = 2^{-1/2} \sum_\sigma |\Phi_\sigma\rangle$ for the required eigenvalue problem, $H|\Phi\rangle = E|\Phi\rangle$, considering a two particle wave function of the form

$$|\Phi_\sigma\rangle = \sum_{jl} \{ \Phi_{jl}^{(1)} b_{j\sigma}^\dagger a_{l,-\sigma}^\dagger + \Phi_{jl}^{(2)} d_{j\sigma}^\dagger c_{l,-\sigma}^\dagger + \Phi_{jl}^{(3)} d_{j\sigma}^\dagger a_{l,-\sigma}^\dagger + \Phi_{jl}^{(4)} b_{j\sigma}^\dagger c_{l,-\sigma}^\dagger \} |0\rangle \ ,$$

where $\Phi_{jl}^{(n)}$ are the four types of probability amplitude for finding an electron at the monomer j and a hole at the monomer l ($j,l = 1,2,\ldots,N$). The eigenvalue problem is therefore

$$\sum_{stm} H_{jln}^{stm} \Phi_{st}^{(m)} = E \Phi_{jl}^{(n)} \ , \tag{9}$$

where the matrix elements of the Hamiltonian H_{jln}^{stm} follow from Eqs. (1), (2), and (3). Obviously, with the dipole-dipole term $V_{12} \equiv V_{xy} = 0$, the x and y channels in the Hamiltonian (1) are decoupled. This is the case we will study in the present paper.

We have solved Eq. (9) and evaluated the conductivity $\mathrm{Re}\sigma_{\alpha\alpha}(0,\omega)$ defined in Eq. (6) for different lengths of model oligomers and different values of the microscopic parameters. Some of our results are presented in Sec. IV and V with the aim of comparing with available experimental data. These results are plotted employing a phenomenological broadening parameter Γ in Eq. (6) which replaces the δ function $\delta(x)$ by the Gaussian $(\sqrt{\pi}\Gamma)^{-1}\exp(-x^2/\Gamma^2)$. In this way continuous absorption bands are obtained which redistribute the oscillator strength of the unbroadened eigenvalues E_κ. Before presenting these results, we note the useful insight that is provided by the following analytical treatment of the infinite chain.

III. ANALYTICAL THEORY FOR THE INFINITE POLYMER CHAIN

For the problem of a *single* electron interacting with a *single* hole the Kubo formulas are readily evaluated in terms of standard ladder diagrams only.[16] These are shown for $\sigma_{xx}(Q,\omega)$ in Fig. 1 (x and y channels are decoupled). The results can be expressed in a closed analytical form if the *long-range* Coulomb interaction V_{eh} is set equal to zero. For σ_{xx} we obtain

$$\sigma_{xx}(Q,\omega)=(e^2/2Abi\omega)[F_x(Q,\omega+i\Gamma)+F_x(-Q,-(\omega+i\Gamma))] .$$

In this section the broadening parameter $\Gamma=\hbar(1/\tau_e+1/\tau_h)$, where τ_e and τ_h are phenomenologically introduced lifetimes of the individual electron and hole states. The function

$$F_x(Q,\omega)=\langle v^2\chi_{ab}\rangle+\langle v^2\chi_{cd}\rangle+D_x^{-1}(f\langle v\chi_{ab}\rangle^2+g\langle v\chi_{cd}\rangle^2+h\langle v\chi_{ab}\rangle\langle v\chi_{cd}\rangle) , \quad (10)$$

where we have introduced the Q- and ω-dependent quantities:

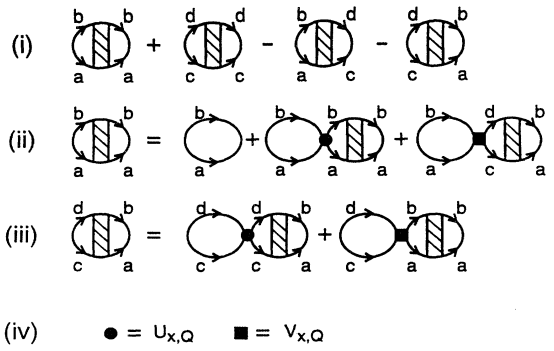

FIG. 1. (i) Feynman diagrams for the calculation of $\sigma_{xx}(Q,\omega)$. (ii) Ladder summation for the first term in (i). (iii) Ladder summation for the fourth term in (i). The second and third terms of (i) are given by ladder summations similar to (ii) and (iii). The vertices $U_{x,Q}$ and $V_{x,Q}$ are defined in the text.

$$D_x=(1-U_{x,Q}\chi_B)(1-U_{x,Q}\chi_D)-(V_{x,Q})^2\chi_B\chi_D , \quad (11)$$

$$\langle v^n\chi_{ab}\rangle=N^{-1}\sum_k v^n_{k,Q}/(2\alpha_0-2E_{k,Q}-\omega) ,$$

$$\langle v^n\chi_{cd}\rangle=v_0^n/(2\alpha_0-\omega) ,$$

$$f=U_{x,Q}(1-U_{x,Q}\langle\chi_{cd}\rangle)+V^2_{x,Q}\langle\chi_{cd}\rangle , \quad (12)$$

$$g=U_{x,Q}(1-U_{x,Q}\langle\chi_{ab}\rangle)+V^2_{x,Q}\langle\chi_{ab}\rangle , \quad (13)$$

$h=2V_{x,Q}$. Here $v_{k,Q}=v_0+2v_1\cos(kb)\cos(Qb/2)$ and $E_{k,Q}=2t\cos(kb)\cos(Qb/2)$. $\sigma_{xx}(Q,\omega)$ describes absorption derived from the $B^\dagger$ and $D^\dagger$ transitions. Correspondingly, the functions $\langle\chi_{ab}\rangle=\chi_B$, $\langle\chi_{cd}\rangle=\chi_D$ in Eqs. (12), (13), and (11) are just the propagators for the $B^\dagger$ and $D^\dagger$ excitations: $\chi_B=[(2\alpha_0-\omega)^2-W_Q^2]^{-1/2}$ and $\chi_D=(2\alpha_0-\omega)^{-1}$. Here $W_Q=W\cos(Qb/2)$ and the bandwidth $W=4t$. The interaction matrix elements are

$$U_{x,Q}=(U_1+U_3)/2+V_{xx}\cos(Qb) ,$$
$$V_{x,Q}=(U_1-U_3)/2+V_{xx}\cos(Qb) . \quad (14)$$

If $V_{x,Q}$ were zero, the $B^\dagger$ and $D^\dagger$-derived excitations would be decoupled. It follows from Eq. (10) that the $B^\dagger$-derived excitations would then consist of a continuum of interband transitions with energies $2\alpha_0-W_Q\le\omega\le2\alpha_0+W_Q$, with an excitonic bound state ("$B^\dagger$ exciton") below this continuum with energy

$$\hbar\omega_{Q,1}=2\alpha_0-(U^2_{x,Q}+W_Q^2)^{1/2} . \quad (15)$$

The fraction of the total oscillator strength of the $B^\dagger$ excitations assumed by this exciton would be $f_Q=U_{x,Q}/(U^2_{x,Q}+W_Q^2)^{1/2}$ (this simple formula is valid for $v_1=0$) and is close to unity for $U_{x,Q}>W\cos(Qb/2)$. As Q increases, therefore, increasingly more oscillator strength would be transferred to the exciton. The $D^\dagger$-derived excitations would consist of a single dispersing Frenkel-like exciton ("$D^\dagger$ exciton") with energy

$$\hbar\omega_{Q,2}=2\alpha_0-U_{x,Q} \quad (16)$$

and one-half of the oscillator strength of the original $E_{1u}(x)$ excitation. In general the two types of excitations are coupled to each other by $V_{x,Q}\neq0$ and lead generically to a *lower*-energy and *higher*-energy absorption band in $\mathrm{Re}\sigma_{xx}(Q,\omega)$. This coupling is reflected in the function D_x, defined in Eq. (11), the zeros of which as a function of ω determine the energies $\hbar\omega_Q$ and lifetimes of the $B^\dagger$ and $D^\dagger$ excitons. For $v_1=0$, the function F_x simplifies and leads to the result given in Ref. 4.

For σ_{yy} the analytical results have been presented in Ref. 4. $\sigma_{yy}(Q,\omega)$ is derived from the $A^\dagger$ and $C^\dagger$ transitions. The matrix elements now are

$$U_{y,Q}=(U_2+U_4)/2+V_{yy}\cos(Qb) ,$$
$$V_{y,Q}=(U_2-U_4)/2+V_{yy}\cos(Qb) .$$

Because the relevant propagators are equal, $\chi_A=\chi_C=[(2\alpha_0-\omega)^2-(W/2)^2]^{-1/2}$, the resulting absorption is not split into higher- and lower-energy bands. This is a consequence of the assumption of charge-conjugation

symmetry. In the limit $\Gamma \to 0$, the original $E_{1u}(y)$ excitation spreads into a continuum of interband excitations with energies $2\alpha_0 - W/2 \leq \omega \leq 2\alpha_0 + W/2$, together with an exciton below this continuum with energy

$$\hbar\omega_{Q,3} = 2\alpha_0 - [\tilde{U}_{g,Q}^2 + (W/2)^2]^{1/2} , \quad (17)$$

where $\tilde{U}_{y,Q} = U_2 + 2V_{yy}\cos(Qb)$. This "$E_{1u}(y)$ exciton" corresponds to a bound state between an extended electron and a localized hole or vice versa. Its energy lies in between those of the $B^\dagger$ and $D^\dagger$ excitons and we refer to it as the "intermediate energy" exciton.

Interestingly, it follows from the function D_y analogous to D_x defined in Eq. (11) (or, alternatively, from the retarded propagator $i\theta(t)\langle\{[P_{j,4}^\dagger(t) - P_{j,4}(t)], [P_{j,4}^\dagger(0) - P_{j,4}(0)]\}\rangle$) that there is a fourth, *dipole-forbidden,* singlet state exciton with energy

$$\hbar\omega_4 = 2\alpha_0 - [U_4^2 + (W/2)^2]^{1/2} . \quad (18)$$

This resides below a continuum of dipole-forbidden interband excitations lying in the same range of energies as the allowed $E_{1u}(y)$-derived interband excitations. These excitations, of course, are simply those derived from the B_{2u} monomer excitation. Note the absence of dispersion in Eq. (18) for $\hbar\omega_4$ which reflects the absence of a transition dipole moment for this exciton under local D_{6h} symmetry. The fourth exciton is *rendered allowed* when CCS is broken, i.e., when $\chi_A \neq \chi_C$.[12]

The four singlet state excitation bands just described are schematically illustrated in Fig. 2 for the ideal case $\Gamma = 0$. The typical ordering of the four exciton levels is $\omega_{Q,1} < \omega_4 < \omega_{Q,3} < \omega_{Q,2}$. Note that the symmetries shown in this figure indicate the symmetries of the *benzene* excitations from which these polymer excitations are *derived.* The polymer excitations themselves in nonplanar PPP belonging to the D_2 point group have B_3 and B_2 symmetry, respectively, for polarizations along and perpendicular to the polymer axis. Note also that with $V_{eh} \neq 0$ more exciton levels, including those of A_g symmetry, would be split from the bands.

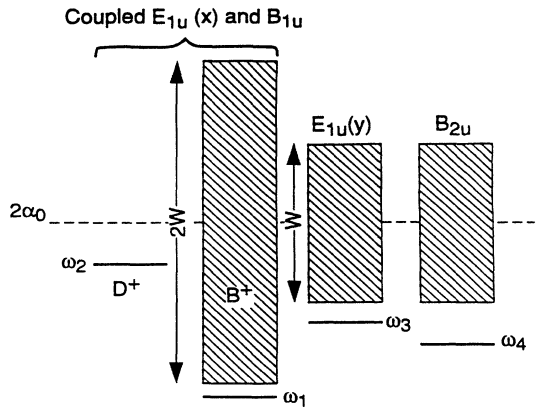

FIG. 2. The four singlet excitation energy bands of the model phenylene polymer. The first two bands are derived from coupled $E_{1u}(x)$ and B_{1u} excitations of benzene while the third and fourth bands are derived from $E_{1u}(y)$ and B_{2u} excitations, respectively. $\omega_1, \omega_2, \omega_3$, and ω_4 denote the four exciton levels while $2\alpha_0$ is the ionization energy minimum the electron affinity for the polymer.

We note that the EELS spectra calculated from $\sigma_{xx}(Q,\omega)$ have been presented in Ref. 4 in which space requirements prevented the function $F(Q,\omega)$ defined in Eq. (10) from being presented.

IV. APPLICATION TO DIMERS

We believe that the origin of the main absorption bands observed in wide-band phenylene-based oligomers and their polarization can be understood already in the one-electron picture. According to Eqs. (7) and (8), transitions $a \to b$ orbitals and $c \to d$ orbitals are polarized along the x axis, while $a \to d$ and $c \to b$ are polarized along the y direction. In an oligomer the a and b states are split by H_d, Eq. (2), while the c and d states remain localized (with the energy α_0). The number of observable optical transitions depends on the number of monomers N. Consider the simplest case $N = 2$. With oblique hops being ignored the split excitation energies are given by $\alpha_0 \mp t$ for "bonding" and "antibonding" excitations, respectively. The parallel polarization should be represented by three peaks (two bonding excitations, two localized ones, and two antibonding excitations) and for perpendicular polarization two peaks are expected (one localized excitation and either a bonding or an antibonding one). These five peaks in order of increasing energy alternate in polarization and would be equidistant at spacing t from each other. In the one-electron model oblique hops can be treated exactly and for the eigenenergies the result is $[(\alpha_0 \mp t)^2 + t^2]^{1/2}$. Obviously, the equidistant picture of transition energies is somewhat distorted by oblique hops. However, the lowest three transition energies are still separated by equal spacings. This is a general property of the one-electron model with CCS since these transitions correspond to the production of two bonding excitations, or one bonding and one localized excitation, or two localized excitations, respectively, and there are only one bonding and one localized value of excitation energy involved. To have this property violated, Coulomb interactions must be taken into account. For moderate magnitudes of correlation energies U_n and large broadening parameter Γ, the effect of the interactions in the spectra is the relative shift of the main absorption bands and redistribution of oscillator strength between them. Such a shift can be seen in Fig. 3 which shows the calculated (in the truncated model) polarized optical absorption of a dimer.

Let us list the parameters one has to specify for a dimer calculation. It is important to notice that in systems with CCS the dipole-allowed absorption spectra are not affected by the value of U_4; see Eq. (17). We take $U_1 = U_2$ and $U_3 - U_1 = 0.8$ eV from the benzene data. Then the relative positions of the absorption peaks are fully determined by t, V, and the difference $U_1 - V_C$. As a trial, we use $V = 0.1$ eV and $U_1 = V_C$. The absolute positions of the peaks may conveniently be determined employing the parameter E_1, the "observable" transition energy for a phenylene monomer. By choosing $t = 0.7$ eV and $E_1 = 6.6$ eV we have calculated the spectrum shown in Fig. 3. (Other parameters involved, but *not* affecting

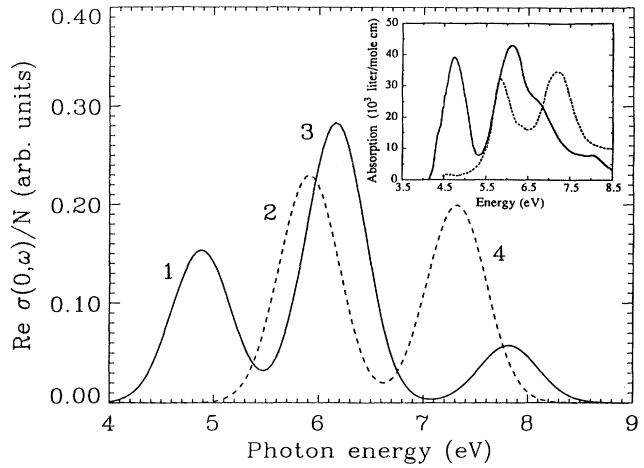

FIG. 3. The calculated absorption spectra of a dimer for light polarized along the x (solid line) and y (dashed line) directions. Here the parameters used are $E_1=6.6$ eV, $t=0.7$ eV, $U_3-U_1=0.8$ eV, $U_1=U_2=V_C$, $V=0.1$ eV, $\Gamma=0.4$ eV, and $v_1/v_0=0.3$. The inset shows the corresponding absorption spectra of a biphenyl crystal taken from Ref. 7.

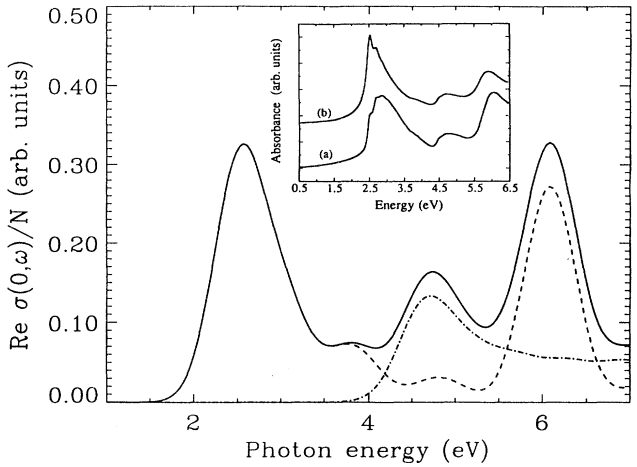

FIG. 4. The calculated absorption spectra of a 10-monomer chain. The dashed line is for the x-polarized absorption, the dash-dotted line is for the y-polarized one, and the solid line gives their sum representing unpolarized absorption. The parameters utilized are $E_1=6.5$ eV, $W=4.1$ eV, $U_3-U_1=0.7$ eV, $U_1=U_2=V_C=0.2$ eV, $V_{xx}=0.1$ eV, $\Gamma=0.4$ eV, and $v_1/v_0=0.5$. The inset shows the absorption spectra of unoriented PPV taken from Ref. 23: curve a, "standard" PPV and curve b, "improved" PPV.

the peak positions, are $\Gamma=0.4$ eV and $v_1/v_0=0.3$.) The resulting absorption band 1–4 in Fig. 3 correspond fairly well to the main experimental absorption peaks of a biphenyl crystal observed in Ref. 7 at 4.80, 5.88, 6.16, and 7.24 eV, as shown in the inset in Fig. 3. (We do not speculate about less pronounced peaks.) It is apparent that for unpolarized light bands 2 and 3 merge and cannot be resolved so that one sees only three main bands, as observed, for instance, in Ref. 7 in the optical spectrum of biphenyl vapor at 5.1, 6.41, and 7.66 eV (see also Ref. 13) and in EELS of biphenyl films.[17] These peak positions of biphenyl vapor are also reasonably well reproduced by our fit if we use the value of $E_1\simeq 6.9$ eV from the benzene vapor spectrum. The blueshift in the transition energy E_1 of the vapor spectrum relative to the crystal can be attributed to polarization effects in the crystal.[13,18] Available data on another dimer-type molecule, stilbene, in solution, reveal three absorption bands with maxima[13] at 4.22, 5.43, and 6.15 eV which we ascribe to bands 1, 2, and 3, respectively. These can also be fit satisfactorily within the same scheme utilizing the value of $t\simeq 1$ eV, $V_{xx}=0.1$ eV, and $U_3-U_1=0.7$ eV. These fits give further evidence that the simplified model we use incorporates the basic features and is sufficient to understand polyphenylene spectrum evolution starting from a phenylene monomer.[19,20]

V. APPLICATION TO LONGER CHAINS

For N larger than 2, new, smaller, peaks appear in the absorption spectra. In Fig. 4 one can distinguish small bumps in addition to the main absorption peaks even in the case of a 10-monomer chain. Of course, the number of possible transitions in the more detailed model of PPV would be larger than the number of transitions in the PPP-type model with the same N. The additional features, caused by finiteness, become less and less resolved as the length increases, as they do also when mixtures of different length chains are considered.

Consider now a long chain of phenylene monomers in the one-electron picture. In the frequency range usually measured (up to about 6.5 eV) one expects transitions between the wide bands of delocalized (a,b) states with a peak at the band edge (an analog to the absorption band 1 above), between a wide band and a flat band of localized (c,d) states (a band-edge peak is analogous to peak 2) and between two flat bands (an analog to peak 3). In fact, a three-peak absorption structure has been observed in PPV (Refs. 5, 21–23, and 25) and interpreted in this way.[5,22] In RG (Ref. 4) (see also Sec. III) polarization assignments of these peaks have been made and, further, it was pointed out that, in a noninteracting system, the intermediate-energy (IE, $\hbar\omega_3$) peak would fall precisely in the middle between the lower- (LE, $\hbar\omega_1$) and higher-energy (HE, $\hbar\omega_2$) ones. The reasoning behind this is the same as in the dimer case discussed above. Displacement of the IE peak from the middle position in the experimental data by itself already indicates the presence of an interaction between an electron and hole, and this is indeed the case in the spectra of PPV. We observe that in the experimental spectra of PPV the IE peak is typically much smaller than the LE and HE peaks (see, e.g., the inset in Fig. 4). Also, and interestingly, both in the EELS (Refs. 2 and 5) and absorption spectra[6] of PPP the IE peak is *apparently* not present. We now find an explanation of these two further observations in the *details* of the effective electron-hole interaction.

From the studies of one-dimensional excitons[26] it is known that the energy and wave function of the excitonic state are sensitively dependent on the potential profile for closely spaced electron and hole. In our model it is the

interplay of the parameters U_n and V_C that determines the behavior of the excitonic wave function near the origin and, hence, the transition intensities. It is instructive to return to the dimer spectrum in Fig. 3 obtained with $U_1=V_C$ (that is, with $E_1=E_{CT}$). Our study has shown that with $U_1>V_C$, the absorption band 3 in this figure would borrow more oscillator strength from band 1, and band 2 would borrow from band 4. The redistribution of the oscillator strength is reversed in the case $U_1<V_C$: $3\rightarrow 1$ and $2\rightarrow 4$. [It is worthwhile to stress that such a relationship between the parameters is quite physical so long as $(\sum_n U_n)/4$ is larger than V_C.] Comparing experimental spectra in Ref. 7 one can observe the tendency for the latter changes in the band intensities on going from the biphenyl vapor to the biphenyl crystal spectrum. This can be understood as a polarization effect—a charge-transfer exciton polarizes the medium more strongly than a Frenkel one, thus in effect increasing V_C more than U_1. We have also found that change of the relative magnitudes of the correlation energies U_n, particularly of U_3 relative to U_1, leads to modifications of the absorption spectra. Specifically, it is the fact that $U_3>U_1$ that makes bands 2 and 3 of the dimer spectrum in Fig. 3 overlap and peak 3 to be of a greater intensity than peak 1. All in all, comparing the calculated and experimental crystal spectra in Fig. 3 one must conclude that the main relationship between the microscopic parameters has been taken more or less correctly.

Figure 4 shows the absorption spectrum of an $N=10$ monomer chain with the trial parameters $W=4t=4.1$ eV, $U_1=U_2=V_C$, $U_3-U_1=0.7$ eV, and $V_{xx}=0.1$ eV inferred from the fit of stilbene data, and using $V_C=0.2$ eV, a reasonable value. With the chosen value of $E_1=6.5$ eV, the spectrum shows three peaks at about 2.6, 4.8, and 6.1 eV which compare well with the experimental PPV data in the inset. Note that now the calculated intensity of the IE peak is lower than the intensities of the LE and HE peaks. This has resulted from choosing a small value of U_2 so that the IE peak does not experience strong excitonic enhancement. At the same time, the HE peak is appreciably shifted downward in energy by the Coulomb interactions: U_1 is small but $(U_1+U_3)/2$, which matters for the HE and LE peaks, Eq. (14), is larger. (The intensity of the LE peak here is enhanced by the oblique transitions for which we have taken $v_1/v_0=0.5$.) This indicates the importance of the fact, deduced from benzene spectroscopic data, that the correlation gaps U_n have markedly different values. Unfortunately, in this parameter range relatively small changes in the peak positions can be caused by considerable modification of the microscopic parameters. Also, the PPP-type model used for calculations is rather a qualitative model when applied to PPV. This prevents us from pinpointing the values of the parameters by precisely fitting the experimental data. In addition, precise fitting makes no sense at the present stage because the peak positions in different samples of PPV differ. [Compare, e.g., curves *a* and *b* in the inset in Fig. 4 and data reported in Refs. 21 and 25.] Nevertheless, the range of parameter values used for Fig. 4 already implies that the lowest exciton is weakly bound in the sense that the bandwidth W is larger than the relevant Coulomb interactions [$(U_1+U_3)/2$ and V_C]. In fact, with the parameter values used for the 10-monomer chain in Fig. 4 the lowest excitation energy is moved down by ~ 0.2 eV with respect to that in a noninteracting system ($U_n=V_C=V_{dd}=0$). To compare, for a 5-monomer chain with the same set of parameters a downward shift ~ 0.3 eV of the lowest excitation energy is obtained. This would suggest an exciton binding energy ~ 0.2–0.3 eV in actual samples with short conjugation lengths. Here the binding energy is understood as necessary to separate electron and hole over distant oligomers. Of course, the Coulomb parameters could be somewhat underestimated here. So in the calculation employing the same parameters as for Fig. 4 but with $U_1=V_c=0.4$ eV and $W=4.2$ eV, the LE peak appears to be shifted to ~ 2.5 eV and the binding energy to be ~ 0.4 eV. On the other hand, one might note that in the truncated model the wide band spectrum is given by the expression

$$\epsilon(k)=\alpha_0-2t\cos(kd) \tag{19}$$

while oblique terms would modify it to

$$\tilde{\epsilon}(k)=[\epsilon^2(k)+4t^2\sin^2(kd)]^{1/2}\ . \tag{20}$$

Making use of the untruncated band spectrum Eq. (20) rather than Eq. (19) would lead to a *decrease* of the band electron effective mass and, hence, to a decrease of the binding energy. We can only conclude therefore that the binding energy of the LE exciton is of the *order* of tenths of eV. In any case, our estimate is inconsistent with the value of 1.1 eV obtained for the binding energy of the LE exciton in Ref. 27 from an interpretation of PPV optical data. It is clear that the IE exciton is also expected to be weakly bound (U_2 is small in comparison with $W/2$). In contrast to these excitons, the HE exciton, $\hbar\omega_2$, and the dipole-forbidden exciton $\hbar\omega_4$ must be tightly bound excitons ($U_4\sim 2$ eV is a big parameter). Clearly, relaxation of the lattice[28] about such excitons, which concentrate loss of bond order over only a very few monomers,[29] is an important consideration. This is also relevant for the triplet excitons described in the Appendix since, based on our estimates, the corresponding correlation energies U_{nt} are comparable to the electronic bandwidth W.

It is interesting to compare Fig. 4 with Fig. 5, in which we used for the calculation of $\sigma(0,\omega)$ the following parameter values: $W=4t=3$ eV, $E_1=6.5$ eV, $U_1=U_2=V_C=0.2$ eV, $U_3-U_1=0.8$ eV, $V=0.1$ eV, $\Gamma=0.45$ eV, and $v_1/v_0=0.3$. Here, the smaller value of t inferred from our fit of the biphenyl is used while the other parameters affecting the peak positions are very close to those used in computing the spectrum of Fig. 4. As a result, in the unpolarized absorption spectrum the IE peak in Fig. 5 becomes hardly resolvable from the HE one. We think this explains why the IE peak has not yet been identified in experiments on PPP.[2,5,6] (Experimental data on the uv spectrum of PPP are scarce compared to PPV.) It is relevant to recall here that the corresponding peaks 2 and 3 in the absorption spectrum of biphenyl vapor *completely* overlap.[7] We therefore expect that the IE peak would be detected if *polarized* spectra of crystalline

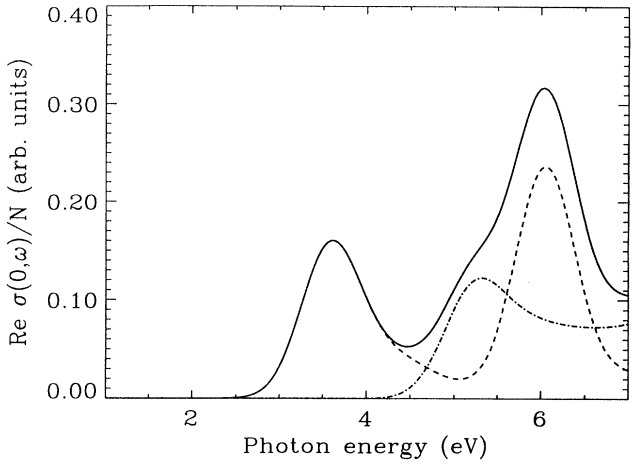

FIG. 5. The same as Fig. 2 but with the following parameters used: $E_1=6.5$ eV, $W=3$ eV, $U_3-U_1=0.8$ eV, $U_1=U_2=V_C=0.2$ eV, $V=0.1$ eV, $\Gamma=0.45$ eV, and $v_1/v_0=0.3$. This spectrum is representative of PPP.

films of PPP could be satisfactorily measured. Thus, at the level of the *effective* model, the main distinction between PPP and PPV is different magnitudes of W. The smaller value corresponding to PPP may be due to nonplanarity of PPP as compared to the nearly planar structure of PPV. In conclusion of this section we note that making use of the Coulomb interaction parameters and W employed here with the analytical formulas of Sec. III produces absorption spectra whose main features are very similar to those in Figs. 4 and 5. In these "analytical" absorption spectra, of course, there are no additional "bumps" due to spatial quantization.

VI. CONCLUSIONS

We have demonstrated that detailed study of the effective electron-hole interaction in the RG model enables one to understand not only the origin, polarization, and positions of the main absorption bands in phenylene-based oligomers but their intensities as well. The agreement between the gross features of the experimental and theoretical spectra attained in Figs. 3 and 4 appears convincing and may thus be considered to provide experimental information on the effective electron-hole interaction in these polyphenylenes. Although we have not yet determined the microscopic parameters characterizing PPV and PPP precisely, we have obtained an idea of their magnitudes from the latter approximate fits. We believe that systematic polarized experiments in uv-visible regions and EELS studies on films of good crystallinity would allow a more precise extraction of the microscopic parameters of the model. It could be very useful to study the evolution of the spectra in a series of oligomers of different lengths from the standpoint of the present approach.[30] The application to derivatized and atomically bridged polyphenylenes of an explicit study of the RG model with electron-hole symmetry broken is presented separately.[12]

APPENDIX: TRIPLET EXCITONS

It is straightforward to extend our model to calculate the energies of the triplet state excitons. To Eq. (3) for H_{ee} we add the following term describing the energy gain U_{nt} when an electron and a hole, in a triplet state, are simultaneously present on the same monomer in the symmetry combination n:

$$-\sum_{jnm} U_{nt} T^{\dagger}_{jnm} T_{jnm} \ . \tag{A1}$$

The operators $T^{\dagger}_{jnm}$ are the triplet state counterparts of the four singlet excitation operators $P^{\dagger}_{jn}$ defined in Sec. II. $m=0,\pm1$ denote the magnetic quantum numbers. The local monomer triplet state excitation energies are then $E_{nt}=2\alpha_0-U_{nt}$. For benzene Salem[8] tabulates $E_{1t}=E_{2t}\simeq4.5$ eV ($^3E_{1u}$), $E_{3t}\simeq3.6$ eV ($^3B_{1u}$), and $E_{4t}\simeq4.7$ eV ($^3B_{2u}$). If we assume the value $2\alpha_0\simeq6.7$ eV in the polymer medium from our calculated absorption spectra in Figs. 4 and 5, we obtain $U_{1t}=U_{2t}\simeq2.2$ eV, $U_{3t}\simeq3.1$ eV, and $U_{4t}\simeq2.0$ eV. These values are significantly larger than the corresponding singlet state values U_n since more work has to be performed to separate a local triplet exciton into a widely spaced electron and hole on account of the exchange interaction. If the long-range Coulomb interaction V_{eh} is neglected, the triplet state T matrix may be calculated analytically from the summation of ladder diagrams. In analogy to the singlet case we find a $B^{\dagger}$-like triplet exciton and a $D^{\dagger}$-like triplet exciton whose energies $\hbar\omega_{1t}(Q)$ and $\hbar\omega_{2t}(Q)$ are given by the solutions of

$$(1-U_{tx}\chi_B)(1-U_{tx}\chi_D)-V^2_{tx}\chi_B\chi_D=0 \tag{A2}$$

and $E_{1u}(y)$- and B_{2u}-derived triplet excitons whose energies $\hbar\omega_{3t}$ and $\hbar\omega_{4t}$ are given by the solutions of

$$(1-U_{2t}\chi_A)(1-U_{4t}\chi_C)=0 \ . \tag{A3}$$

In Eqs. (A2) and (A3) χ_B, χ_D, and $\chi_A=\chi_C$ are the propagators already introduced for the singlet excitations, while

$$U_{tx}=(U_{1t}+U_{3t})/2 \ ,$$
$$V_{tx}=(U_{1t}-U_{3t})/2 \ .$$

It follows immediately from Eq. (A3) that

$$\hbar\omega_{3t}=2\alpha_0-[U^2_{2t}+(W/2)^2]^{1/2} \ ,$$
$$\hbar\omega_{4t}=2\alpha_0-[U^2_{4t}+(W/2)^2]^{1/2} \ .$$

Both of these energies are independent of wave vector Q. Equation (A2) shows that the actual $B^{\dagger}$ and $D^{\dagger}$ triplet excitations are coupled via the matrix element V_{tx}. In the absence of this coupling ($U_{1t}=U_{3t}$) we have

$$\hbar\omega_{1t}(Q)=2\alpha_0-(U^2_{1t}+W^2_Q)^{1/2} \ ,$$
$$\hbar\omega_{2t}=2\alpha_0-U_{1t} \ .$$

As mentioned in the text, since the U_{nt} are comparable to W all four of the triplet excitons are expected to be tightly bound and to be accompanied by lattice relaxation. Using the estimated values of U_{nt} and the value $W \simeq 4.1$ eV appropriate for PPV in Eq. (A2), we calculate the *absolute* energy of the LE triplet exciton to be $\simeq 1.8$ eV and its *binding* energy to be $\simeq 0.8$ eV.

*Also at Department of Thermal Physics, Uzbekistan Academy of Sciences, Katartal 28, Tashkent 700135, Uzbekistan.

†Permanent address: Xerox Corp., Wilson Center, Mail Stop 114-39D, Webster, NY 14580.

[1]For a review, see, e.g., R. L. Elsenbaumer and L. W. Shacklette, in *Handbook of Conducting Polymers,* edited by T. A. Skotheim (Dekker, New York, 1986), Vol. 1, pp. 213–263.

[2]G. Creceliue *et al.*, Phys. Rev. B **28**, 1802 (1983).

[3]J. L Brédas *et al.*, J. Chem. Phys. **76**, 3673 (1982); **77**, 371 (1982).

[4]M. J. Rice and Yu. N. Gartstein, Phys. Rev. Lett. **73**, 2504 (1994).

[5]J. Fink, Synth Met. **21**, 87 (1987); J. Fink *et al.*, in *Electronic Properties of Conducting Polymers,* edited by H. Kuzmany, M. Mehring, and S. Roth (Springer, Berlin, 1987); E. Pellegrin *et al.*, Synth. Met. **41**, 1353 (1991).

[6]C. Ambrosch-Draxl *et al.*, Synth. Met. **69**, 411 (1995). Unfortunately, the important question of the anisotropy of the uv optical absorption is not explicitly discussed in this paper.

[7]T. G. McLaughlin and L. B. Clark, Chem. Phys. **31**, 11 (1978).

[8]L. Salem, *The Molecular Orbital Theory of Conjugated Systems* (Benjamin, Reading, MA, 1966).

[9]M. Goeppert-Mayer and A. L. Sklar, J. Chem. Phys. **6**, 645 (1938).

[10]C. B. Duke and W. K. Ford, Int. J. Quantum Chem. Quantum Chem. Symp. **17**, 597 (1983).

[11]This is also clearly seen in the electronic structure of PPV calculated by VEH (valence effective Hamiltonian) method, see Fig. 5 in F. Meyers, A. J. Heeger, and J. L. Brédas, J. Chem. Phys. **97**, 2750 (1992).

[12]Yu. N. Gartstein, M. J. Rice, and E. M. Conwell, Phys. Rev. B **51**, 5546 (1995). [MEH refers to the two substituents (2-methoxy) and (5-(2′-ethyl)-hexoxy).]

[13]H. Suzuki, *Electronic Absorption Spectra and Geometry of Organic Molecules* (Academic, New York, 1967).

[14]See also, *Organic Molecular Photophysics,* edited by J. B. Birks (Wiley, London, 1975), Vol. 2; G. Herzberg, *Molecular Spectra and Molecular Structure* (Nostrand, Princeton, 1966), Vol. 3.

[15]I. Egri, J. Phys. C **12**, 1843 (1979); see also T. Hibma *et al.*, Chem. Phys. Lett. **23**, 21 (1973).

[16]See, e.g., G. D. Mahan, *Many Particle Physics* (Plenum, New York, 1981), pp. 730–738.

[17]M. G. Ramsey, D. Steinmüller, and F. P. Netzer, Phys. Rev. B **42**, 5902 (1990).

[18]See, e.g., V. M. Agranovich and M. D. Galanin, *Electronic Excitation Energy Transfer in Condensed Matter* (North-Holland, Amsterdam, 1982). For excitons, this effect arises because of intermolecular interactions, particularly due to different medium polarization by a molecule in the ground and excited states. The calculations in Ref. 7 of lattice dipole-dipole sums show that the crystal interactions do not modify the band assignments for biphenyl.

[19]Applied to such short oligomers as dimers our approach is similar to the so-called composite-molecule method [see H. C. Longuet-Higgins and J. N. Murrell, Proc. Phys. Soc. London Sect. A **68**, 601 (1955) and Ref. 13]. It is noteworthy that with only the few Hamiltonian matrix elements we use the biphenyl main absorption bands can be readily interpreted, whereas much poorer agreement is seen between experiment and theoretical results collected in Ref. 7.

[20]For a comparison of results of different Pariser-Parr-Pople calculations and Hückel theory on stilbene, see Z. G. Soos *et al.*, Phys. Rev. B **47**, 1742 (1993).

[21]J. Obrzut and F. E. Karasz, J. Chem. Phys. **87**, 2349 (1987).

[22]D. D. C. Bradley, J. Phys. D **20**, 1389 (1987).

[23]D. A. Halliday *et al.*, Synth. Met. **55-57**, 954 (1993).

[24]J. Cornil *et al.*, Chem. Phys. Lett. **223**, 82 (1994).

[25]See also N. F. Colaneri *et al.*, Phys. Rev. B **42**, 11 670 (1990); B. R. Hsieh, Polym. Bull. **25**, 177 (1991); J. Bullot, B. Dulieu, and S. Lefrant, Synth. Met. **61**, 211 (1993).

[26]See T. Ogawa and T. Takagahara, Phys. Rev. B **44**, 8138 (1991); S. Abe, in *Relaxation in Polymers,* edited by T. Kobayashi (World Scientific, Singapore, 1993), and references therein.

[27]J. M. Leng *et al.*, Phys. Rev. Lett. **72**, 156 (1994).

[28]S. A. Brazovskii and N. N. Kirova, Pis'ma Zh. Eksp. Teor. Fiz. **33**, 6 (1981) [JETP Lett. **33**, 4 (1981)].

[29]M. J. Rice and S. R. Phillpot, Phys. Rev. Lett. **58**, 937 (1987).

[30]Compare to the analysis of Ref. 24, where the optical absorption spectra of short PPV oligomers are calculated by means of the INDO-SCI (intermediate neglect of differential overlap–single configuration interaction) technique. They do not discuss polarization assignments and the relation of the absorption spectra to the electron-hole interaction.